

## Electronic Supplementary Information (ESI)

### Redirecting Electron Flows in Glutamate Oxidases by Selective Anchoring of Osmium Complexes

Minjung Han,<sup>a†</sup> Sun-Heui Yoon,<sup>a†</sup> Jaehee Lee,<sup>a</sup> Taek Dong Chung,<sup>ab\*</sup> Woon Ju Song<sup>a\*</sup>

<sup>a</sup>Department of Chemistry, Seoul National University, Seoul 08826, Republic of Korea

<sup>b</sup>Advanced Institutes of Convergence Technology, Suwon-Si, Gyeonggi-do 16229, Republic of Korea

\*Email: tdchung@snu.ac.kr, woonjusong@snu.ac.kr

## Methods and Materials

**General procedure.** All solvents and reagents were purchased from Sigma-Aldrich, Acros Organics, TCI Chemicals, or LPS and were used without further purification. NMR spectra were recorded on an Agilent 400 MHz or Bruker 500 MHz NMR spectrometer. UV–Vis spectra were obtained using an Agilent Cary 8454 spectrophotometer. Cyclic voltammetry measurements were performed using an Autolab PGSTAT204 potentiostat. HPLC analysis was conducted on an Agilent 1260 Infinity II or 1220 Infinity II equipped with an InfinityLab Poroshell column (120 EC-C18 4.6 x 100 mm 2.7 microns or 120 EC-C18 4.6 x 150 mm 2.7 microns). Low-resolution LC–MS spectra were obtained using a Thermo Scientific LTQ XL linear ion trap mass spectrometer. High-resolution LC–MS spectra were obtained by an AB SCIEX Q-TOF 5600 mass spectrometer. Osmium concentrations were determined by Perkin Elmer Avio 220 Max ICP-OES spectrometer.

**Synthesis of Os<sup>II</sup>(dmbpy)<sub>2</sub>Cl<sub>2</sub>.** To an oven-dried round-bottom flask equipped with a stir bar, (NH<sub>4</sub>)<sub>2</sub>[OsCl<sub>6</sub>] (1 equiv, 0.68 mmol, 300 mg), 4,4'-dimethyl-2,2'-bipyridine (dmbpy, 2.1 equiv, 1.44 mmol, 264.8 mg), and ethylene glycol (9 mL) were added (Scheme S1). The flask was evacuated and backfilled with argon three times, then refluxed at 190 °C for 1 h under an argon atmosphere. After cooling to room temperature, 1 M Na<sub>2</sub>S<sub>2</sub>O<sub>4</sub> (20 mL) was slowly added to the flask in an ice bath. The resulting dark violet-black precipitate was filtered and washed sequentially with water (5 mL x 3) and diethyl ether (5 mL x 3). The crude product was used without further purification or characterization. Yield: 380.3 mg, 88.5 %.

**Synthesis of [Os<sup>II</sup>(dmbpy)<sub>2</sub>(phen-epoxide)<sub>2</sub>]2PF<sub>6</sub> (OsE).** To an oven-dried round-bottom flask charged with a stir bar, Os<sup>II</sup>(dmbpy)<sub>2</sub>Cl<sub>2</sub> (1 equiv, 0.031 mmol, 19.8 mg), 5,6-epoxy-5,6-dihydro-[1,10]phenanthroline (phen-epoxide, 1.35 equiv, 0.043 mmol, 8.4 mg), and a solution of

EtOH/water (% v/v =75/25) (8 mL) were added (Scheme S1). The flask was evacuated and backfilled with argon three times, then refluxed at 100 °C for 3 h under an argon atmosphere in the dark. After cooling to room temperature, EtOH was removed under reduced pressure. DCM was added to the solution for washing, followed by extraction with water (50 mL x 3). Subsequently, 1 g of NH<sub>4</sub>PF<sub>6</sub> dissolved in H<sub>2</sub>O was slowly added to the flask in an ice bath. The resulting dark brown precipitate was filtered and washed sequentially with water (5 mL x 3) and diethyl ether (5 mL x 3). The crude product was purified by HPLC using acetonitrile as the eluent. OsE was co-isolated with Os(dmbpy)<sub>2</sub>(phen), as similarly reported previously,<sup>1</sup> in a ratio of approximately 2:1. Because the latter species is inert to covalent anchoring to GlutOx, the mixture was used for bioconjugation without further purification.

<sup>1</sup>H NMR (400 MHz, CD<sub>3</sub>CN) δ 8.35 (dd, *J* = 16.7, 8.0 Hz, 6H), 8.12 (d, *J* = 7.9 Hz, 2H), 7.77 (d, *J* = 5.4 Hz, 1H), 7.63 (d, *J* = 5.1 Hz, 1H), 7.49 (d, *J* = 6.0 Hz, 1H), 7.46–7.40 (m, 3H), 7.36–7.31 (m, 1H), 7.19 (t, *J* = 5.8 Hz, 2H), 7.15 (d, *J* = 6.3 Hz, 1H), 4.94 (s, 2H), 2.64 (s, 3H), 2.63 (s, 3H), 2.60 (s, 3H), 2.59 (s, 3H).

LC-MS (ESI, m/z) for C<sub>36</sub>H<sub>32</sub>N<sub>6</sub>OOs calculated = 756.23, observed = 755.24.

**Synthesis of [Os<sup>II</sup>(dmbpy)<sub>2</sub>(bpy-maleimide)](TFA)<sub>2</sub> (OsM).** To an oven-dried round-bottom flask equipped with a stir bar, Os<sup>II</sup>(dmbpy)<sub>2</sub>Cl<sub>2</sub> (1 equiv, 0.0079 mmol, 5 mg), 1-([2,2'-bipyridin]-5-ylmethyl)-1H-pyrrole-2,5-dione (bpy-MI, 1.3 equiv, 0.0103 mmol, 2.74 mg), and a solution of EtOH/water (% v/v =75/25) (12 mL) were added (Scheme S1). The flask was sealed with a septum and copper wire, evacuated, and backfilled with argon three times. The mixture was heated to 92 °C in an oil bath for 5 h. After cooling to room temperature, the crude product was purified by HPLC using 0.1 % TFA in acetonitrile as the eluent. Yield: 3 mg, 34 %.

**<sup>1</sup>H NMR** (400 MHz, (CD)<sub>3</sub>CN) δ 8.41 (dd, *J* = 15.4, 8.3 Hz, 2H), 8.33 (t, *J* = 5.8 Hz, 4H), 7.81 (t, *J* = 7.8 Hz, 1H), 7.70 (d, *J* = 7.0 Hz, 1H), 7.64 (d, *J* = 5.7 Hz, 1H), 7.50–7.44 (m, 3H), 7.43–7.38 (m, 3H), 7.27 (t, *J* = 6.6 Hz, 1H), 7.17 (d, *J* = 5.5 Hz, 2H), 7.13 (s, 2H), 6.78 (s, 1H), 4.55 (dd, *J* = 39.8, 16.2 Hz, 2H), 2.66 (s, 3H), 2.62 (s, 3H), 2.61 (s, 6H).

**LC-MS** (ESI, *m/z*) for C<sub>39</sub>H<sub>35</sub>N<sub>7</sub>O<sub>2</sub>Os calculated = 825.25, observed: 824.39.

**Synthesis of [Os(bpy)<sub>3</sub>](TFA)<sub>2</sub>.** [Os(bpy)<sub>3</sub>]<sup>2+</sup> complex was prepared as reported previously.<sup>2</sup> In short, to an oven-dried round-bottom flask equipped with a stir bar, ammonium hexachloroosmate(IV) (1 equiv, 0.11 mmol, 50.4 mg), 2,2'-bipyridine (bpy, 3.3 equiv, 0.38 mmol, 58.9 mg), and ethylene glycol (9 mL) were added. The flask was evacuated and backfilled with argon three times and refluxed at 190 °C for 1 h under argon atmosphere. After cooling to room temperature, the crude product was purified by HPLC using 0.1 % TFA in acetonitrile as the eluent. Yield: 33.1 mg, 32.6 %. The NMR spectrum is consistent with previous data.<sup>2</sup>

**LC-MS** (ESI, *m/z*) for C<sub>30</sub>H<sub>24</sub>N<sub>6</sub>O<sub>s</sub> calculated = [M]<sup>+</sup> = 660.17, observed: 660.33.

**Molecular Cloning.** The gene for GlutOx (PDB code 2E1M) was synthesized after codon optimization for heterologous expression in *E. coli* (Gene Universal) (Table S1). The gene fragment was inserted into the plasmid pET26b(+) using NdeI and NotI cut sites to yield a plasmid, pET26b(+)/2E1M. For site-directed mutagenesis, custom-made primers were designed as listed in Table S2. All PCR products were conducted with KOD plus new polymerase kit (Toyobo) followed by DpnI digestion and transformed into *E. coli* DH5α competent cells. After digestion with DpnI restriction enzyme for 1.5 h at 37 °C, the plasmids were transformed into *E. coli* DH5α competent cells. Each colony was inoculated in 5 mL LB media with 50 mg/L kanamycin at 37 °C, and the plasmids were extracted for sequencing (Macrogen).

**Preparation and characterization of GlutOx and mutants.** The plasmid pET26b(+)/2E1M was transformed into *E. coli* BL21 (DE3) competent cells containing the pGro7 chaperone plasmid for protein expression, and plated on LB agar plate supplemented with 50 µg/L kanamycin and 34 µg/ml chloramphenicol. A few colonies of BL21 (DE3) containing pGro7 and pET26b(+)/2E1M were grown in 10 ml of LB containing 35 µg/mL chloramphenicol and 50 µg/mL kanamycin at 37 °C with shaking at 150 rpm for 9 h. Following this, 10 mL of the cell culture was inoculated into 1 L of TB containing the same antibiotics, and the cells were grown at 37.5 °C with shaking until the OD<sub>600</sub> reached 1.0–1.2. The temperature was then reduced to 15 °C, and L-arabinose (2 g/L), isopropyl β-D-1-thiogalactopyranoside (IPTG, 0.1 mM) were added. After 18 h, the cells were harvested by centrifugation at 4715 x g at 4 °C for 10 min and stored at –80 °C.

Cell pellets were suspended in 50 mM Tris/HCl buffer containing 250 mM NaCl at pH 7.5 and lysed using an ultrasonic processor (US/VCS750) in an ice bath, with on/off cycles of 3.3 s/3.3 s for 30 min. Cell debris was removed by centrifugation at 18800 × g for 50 min at 4 °C. The resulting supernatants were syringe-filtered and loaded onto a 5 mL HisTrap FF affinity column equilibrated with the same buffer using an ÄKTA pure chromatography system (GE Healthcare) at 4 °C. The protein was eluted using a linear gradient of up to 500 mM imidazole (Figure S3). Further purification was performed using size exclusion chromatography (HiLoad 16/600 Superdex<sup>TM</sup> 200 pg from GE Healthcare) equilibrated with the same buffer to isolate the protein as a dimer.

**Determination of GlutOx concentration.** The FAD content of GlutOx was determined using HPLC and UV-Vis spectroscopy. To extract FAD cofactor, the wild-type enzyme solution was incubated in boiling water for 10 min to denature the protein, and the resulting precipitate was removed by centrifugation, as reported previously.<sup>3</sup> The FAD content in the supernatant was

quantified by reverse-phase HPLC using a C<sub>18</sub>-silica column. A standard curve was generated using free FAD, and the FAD content in the supernatant was calculated accordingly (Figure S4). The extinction coefficient ( $\epsilon_{450}$ ) of FAD in GlutOx was then determined spectroscopically by comparing the UV-Vis absorbance of the enzyme solution with the FAD content obtained from the HPLC analysis, using the following equation,  $A_{450\text{ nm, total}} = A_{450\text{ nm, FAD}} = \epsilon_{450\text{ nm, FAD}} \times [\text{FAD}]$ .

**Bioconjugation of osmium mediator to GlutOx.** To 18 mL of ice-cooled 100 mM Tris/HCl buffer at pH 8.2, 700  $\mu\text{L}$  of the osmium mediator (OsE or OsM, 1 mM, dissolved in DMF) was added at 4 °C. To the resulting solution, 187  $\mu\text{L}$  of protein (1 mM, dissolved in 50 mM Tris/HCl buffer containing 250 mM NaCl, pH 7.5) was added in the presence of 100  $\mu\text{M}$  tris(2-carboxyethyl)phosphine hydrochloride (TCEP) to reduce cysteine residues within GlutOx. The mixture was incubated overnight at 4 °C. Excess mediators and DMF were removed by buffer exchange with 50 mM Tris/HCl buffer containing 250 mM NaCl (pH 7.5) using centrifugal filters (Amicon Ultra). The concentration of the resulting protein-mediator conjugate solution was determined using the extinction coefficient of the protein-bound Os mediators, calculated from UV-Vis spectrophotometry and inductively coupled plasma atomic emission spectroscopy (ICP-OES) analysis (Table S3), using the following equations,  $A_{600\text{ nm, total}} = A_{600\text{ nm, Os}} = \epsilon_{600\text{ nm, Os}} \times [\text{Os}]$ ,  $A_{450\text{ nm, total}} = A_{450\text{ nm, FAD}} + A_{450\text{ nm, Os}} = \epsilon_{450\text{ nm, FAD}} \times [\text{FAD}] + \epsilon_{450\text{ nm, Os}} \times [\text{Os}]$ .

**Biochemical characterizations of GlutOx.** The continuous kinetic activity assay using horseradish peroxidase (HRP) was conducted with a microplate reader (Synergy H1, Biotek), while the discontinuous endpoint assay was performed using an Agilent Cary 8454 spectrophotometer. Hydrogen peroxide (H<sub>2</sub>O<sub>2</sub>) production was performed using an HRP and *o*-dianisidine (*o*-DNS) coupled assay. The enzyme reaction was proceeded in 0.1 M Tris/HCl buffer at pH 7.4, containing 1 mM *o*-DNS dihydrochloride, 1 U/mL HRP (Sigma Aldrich), 20 mM L-

glutamic acid monosodium salt hydrate, and 1 nM enzyme at final concentrations. The reaction was conducted at 30 °C for 15 min. Kinetic activity assay was calculated from the initial rate of absorbance change at 440 nm (oxidized *o*-DNS,  $\epsilon_{440 \text{ nm}} = 13000 \text{ cm}^{-1}\text{M}^{-1}$ ). For the endpoint assay, the formation of H<sub>2</sub>O<sub>2</sub> was quantified by measuring the difference between the final and initial absorbance at 440 nm.

The discontinuous assay to detect  $\alpha$ -ketoglutarate was performed using 3-methyl-2-benzothiazolinone hydrazone (MBTH) method. An enzyme reaction was proceeded in 0.1 M Tris/HCl buffer at pH 7.4, containing 20 mM l-glutamic acid monosodium salt hydrate, and 1 nM enzyme at final concentrations. The reaction was conducted at 30 °C for 15 min and then stopped by adding 2.3% trichloroacetic acid to the reaction mixture. Then, 1 M acetate (pH 5.0) buffer and 9 mM MBTH hydrochloride hydrate (dissolved in 10% DMSO, 0.1 M Tris/HCl pH 7.4) were added to the mixture, which was then incubated at 50 °C for 30 min. After cooling the mixture to room temperature for 30 min, the formation of MBTH-azine  $\alpha$ -ketoglutaric acid was quantified by measuring the difference in absorbance at 368 nm. The extinction coefficient of MBTH-azine  $\alpha$ -ketoglutaric acid ( $\epsilon_{368 \text{ nm}}$  value of  $4000 \text{ cm}^{-1}\text{M}^{-1}$  was determined using HPLC and UV-Vis spectrophotometry.

**Dynamic light scattering (DLS).** The hydrodynamic diameter of the wild-type GlutOx was determined by dynamic light scattering using a Zetasizer (Malvern, Zetasizer Nano ZS) with a disposable micro cuvette (Malvern, ZEN0040). Protein samples (20  $\mu\text{M}$ ) in 50–100  $\mu\text{L}$  were centrifuged at 13 k rpm, 4 °C for at least one hour prior to DLS experiments. GlutOx samples were prepared in 50 mM Tris/HCl 250 mM NaCl (pH 7.5) buffer. The experiment was performed at 25 °C at a detection angle of 173°. The experimental data were analyzed using Zetasizer Software v.8.02 to obtain the intensity profiles.

**Cyclic voltammetry (CV).** Cyclic voltammograms were obtained using an Autolab PGSTAT204 potentiostat and processed by NOVA software. Cyclic voltammetry experiments were conducted in an anaerobic chamber (COY Laboratory Products). All solutions used in the electrochemical experiments were prepared with ddH<sub>2</sub>O and degassed or purged with argon. A three-electrode system was used, consisting of a glassy carbon working electrode (ALS-002012), an Ag/AgCl reference electrode (CHI111), and a platinum wire counter electrode. Cyclic voltammograms were recorded at a sweep rate of 2–100 mV/s, cycling between 0.2 V and 0.9 V, with all potentials referenced to the Ag/AgCl electrode.

For catalytic current measurements, the minimum enzyme concentration of 10 μM was applied to produce a detectable faradaic current above a signal-to-noise ratio of 3, while also minimizing electrode fouling from protein adsorption. The substrate concentration was selected to ensure steady-state catalysis, requiring levels higher than the Michaelis constant ( $K_M$ ) of GlutOx. Therefore, the substrate concentration was set to 200 mM throughout this study.

**Electrochemical analysis of intermolecular electron transfer.** For intermolecular electron transfer between enzyme and mediator, the ratio of steady-state catalytic current ( $i_p$ ) and peak diffusion current of mediator ( $i_p^0$ ) can be derived as reported previously.<sup>4</sup>



$$\frac{i_p}{i_p^0} \approx \frac{\sqrt{\lambda}}{0.446} \sqrt{\frac{2}{\sigma} \left[ 1 - \frac{1}{\sigma} \ln(1 + \sigma) \right]}$$

$$\lambda = \frac{2k_{ET}[E]RT}{Fv}$$

$$\sigma = \frac{k_{ET}[M]}{k_2} \left( 1 + \frac{k_{-1} + k_2}{k_1[S]} \right)$$

$F$  is Faraday's constant,  $A$  is the electrode surface area,  $R$  is the gas constant,  $T$  is the temperature,  $D_M$  is the diffusion coefficient of mediator,  $k_1, k_{-1}, k_2, k_{et}$  are the rate constants shown in the reactions 1 and 2,  $\nu$  is the scan rate,  $[E], [M], [S]$  are the bulk concentrations of the enzyme, mediator, substrate, respectively.

When the rate determining step is the reaction 2 (MET) ( $k_1, k_2 \gg k_{ET}$ ), and substrate saturation is reached ( $k_1 \gg k_{-1}$ ),  $\sigma$  reaches zero, and the equation shown above can be simplified as,

$$\frac{i_p}{i_p^0} \approx \frac{\sqrt{\lambda}}{0.446}$$

Thus, a linear plot of  $\frac{i_p}{i_p^0}$  vs  $\sqrt{\frac{2[E]RT}{F\nu}}$  enables us to estimate  $k_{ET}$  from the slope.

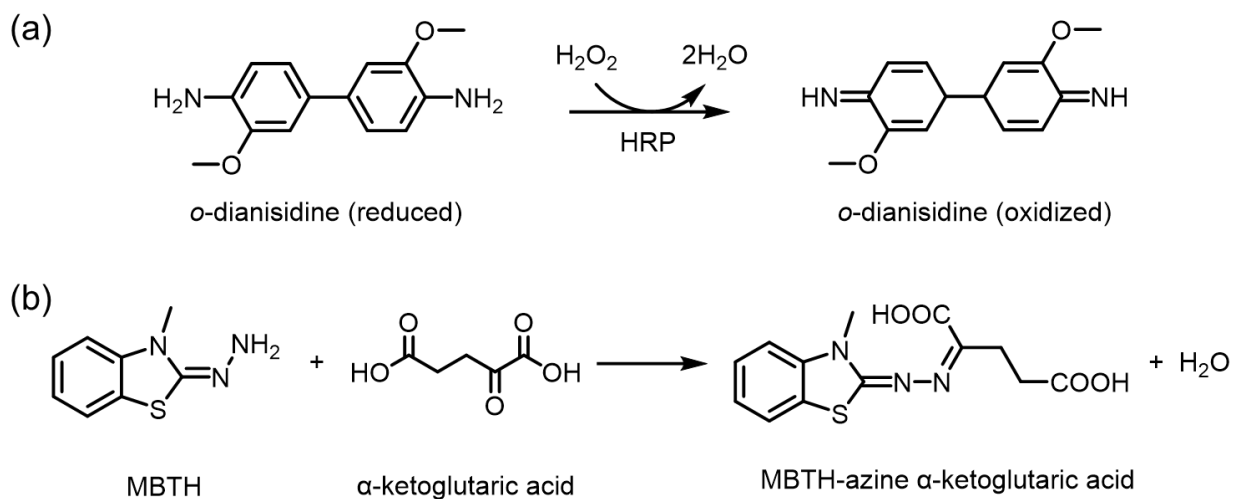
Alternatively, the peak diffusion current ( $i_p^0$ ) of mediator undergoing reversible  $1e^-$  electron transfer can be determined, and  $k_{ET}$ , representing electron transfer between mediator and enzyme can be roughly estimated from  $i_p$  alone, as shown previously.<sup>5</sup>

$$i_p^0 = 0.446FA[M] \sqrt{\frac{D_M F \nu}{RT}}$$

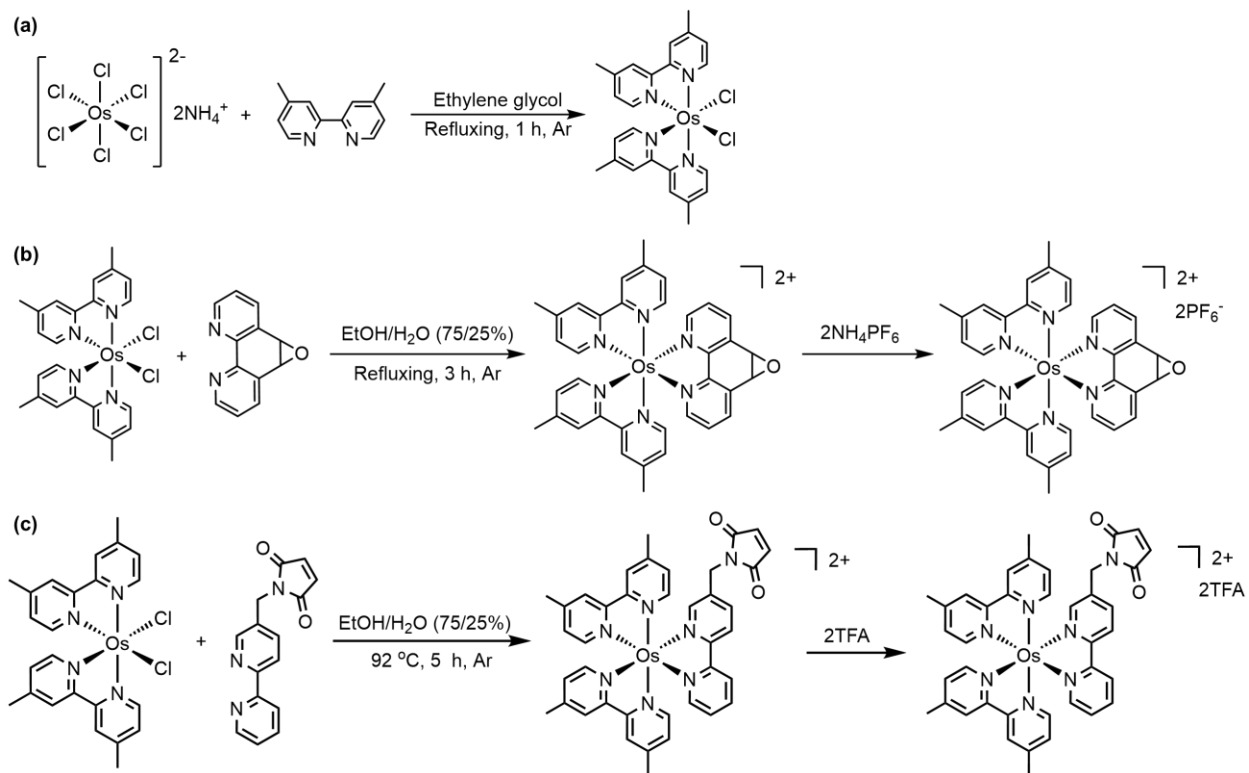
Therefore, the steady-state catalytic current ( $i_p$ ) can be measured as follows.

$$i_p \approx FA[M] \sqrt{2D_M k_{ET}[E]}$$

**Scheme S1.** The reactions used in this work. (a) Continuous HRP assay for H<sub>2</sub>O<sub>2</sub> detection. (b) Discontinuous MBTH assay for  $\alpha$ -ketoglutaric acid detection.



**Scheme S2.** A synthetic scheme of Os complexes used in this work. The preparation of (a)  $\text{Os}(\text{dmbpy})_2\text{Cl}_2$  (b) OsE (c) OsM.



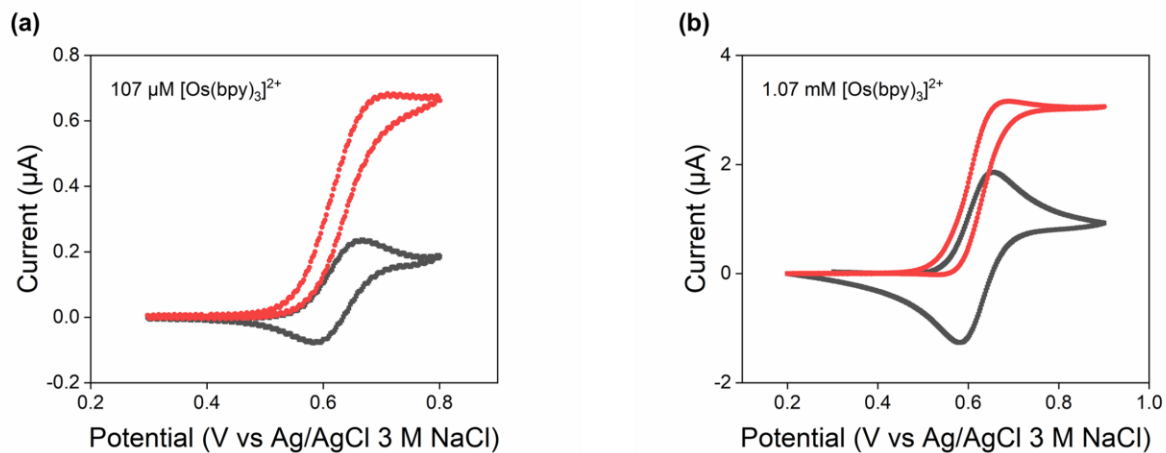
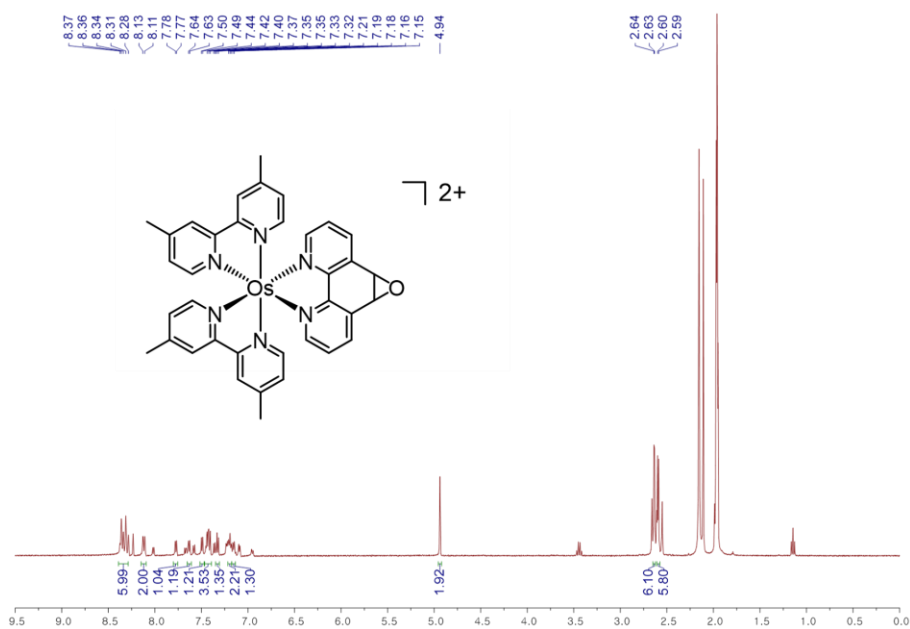


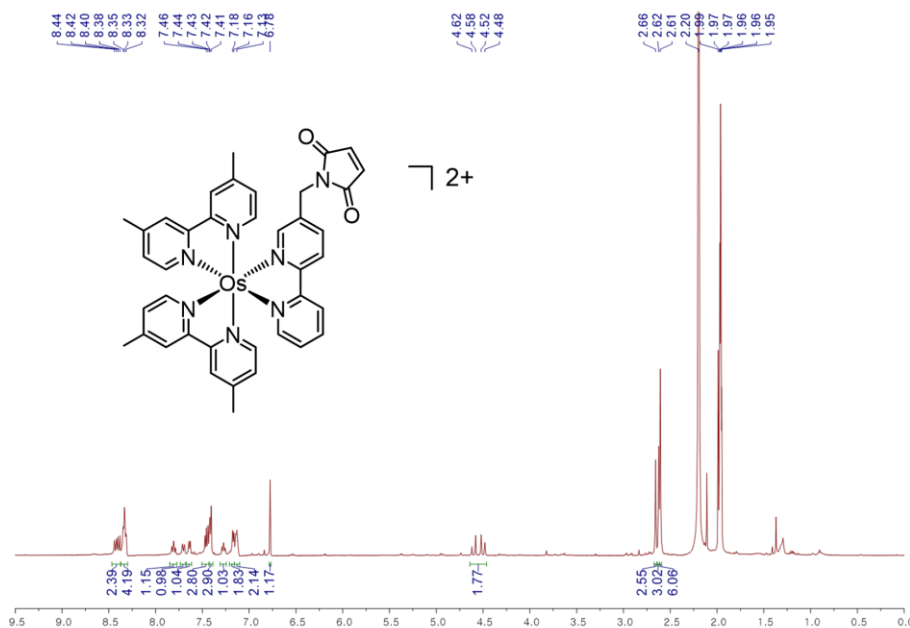
**Fig. S1.** Cyclic voltammograms of catalytic current for the wild-type GlutOx (10 μM) in the presence of (a) 107 μM and (b) 1.07 mM [Os(bpy)<sub>3</sub>]<sup>2+</sup> in DPBS (pH 7.0) (scan rate: 2 mV/s). The black curves represent the diffusion-limited current of [Os(bpy)<sub>3</sub>]<sup>2+</sup> containing L-glutamate (200 mM). The red curves represent the steady-state catalytic current after the addition of wild-type GlutOx (10 μM).

(a)  $^1\text{H}$  NMR of OsE\*

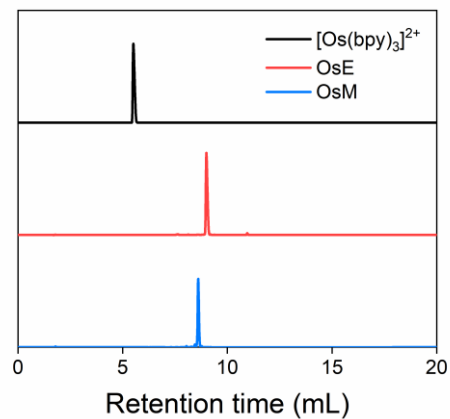


\* The sample contains ca. 30% impurity, presumed to be  $[\text{Os}(\text{dmbpy})_2(\text{phen})]2\text{PF}_6$  determined from LC-MS analysis.

(b)  $^1\text{H}$  NMR of OsM



(c) HPLC



(d) LC-MS

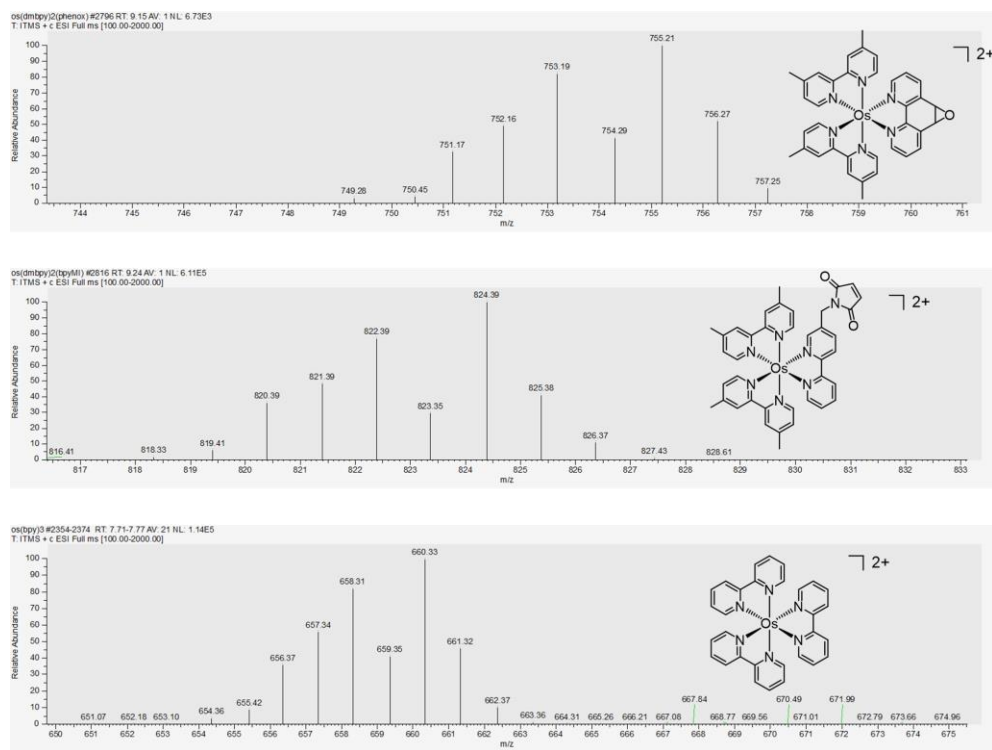


**Fig. S2.** Characterizations of Os complexes used in this work. (a)-(b) <sup>1</sup>H NMR (c) HPLC (d) LC-MS.

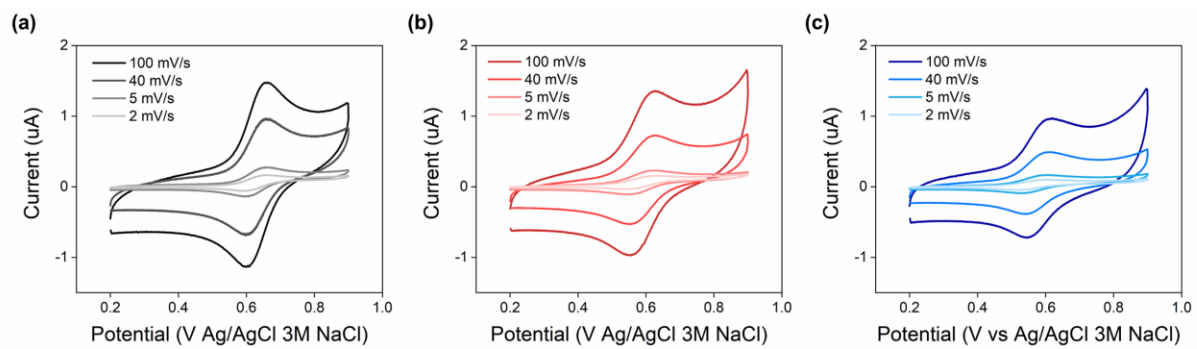


**Fig. S3.** Cyclic voltammograms of the Os complexes (100  $\mu$ M) in DPBS (pH 7.4) at various scan rates.

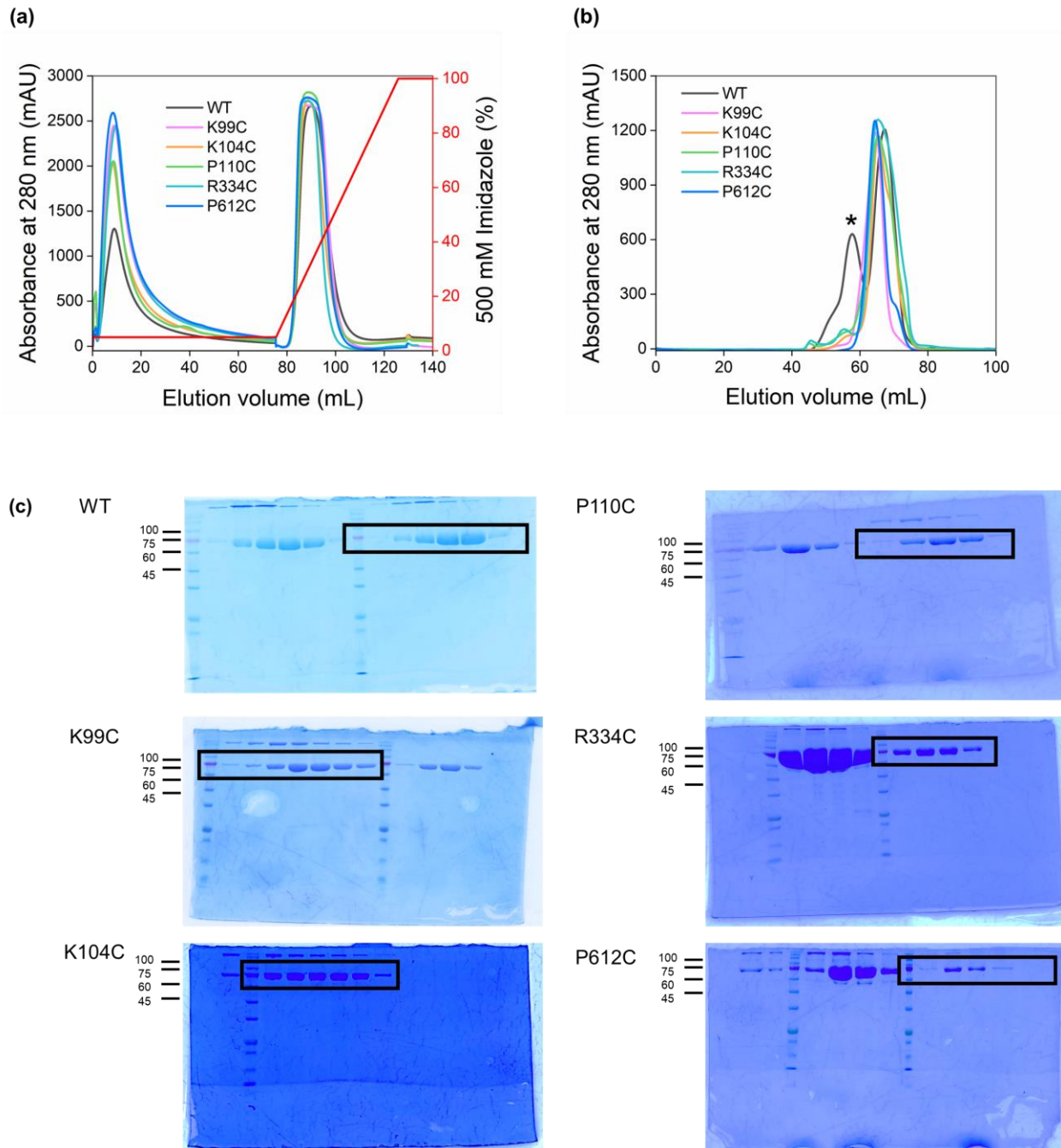
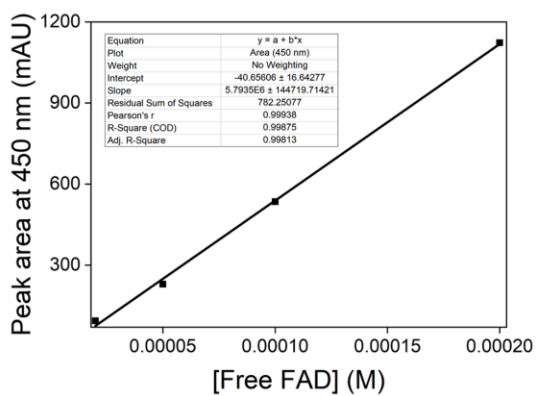
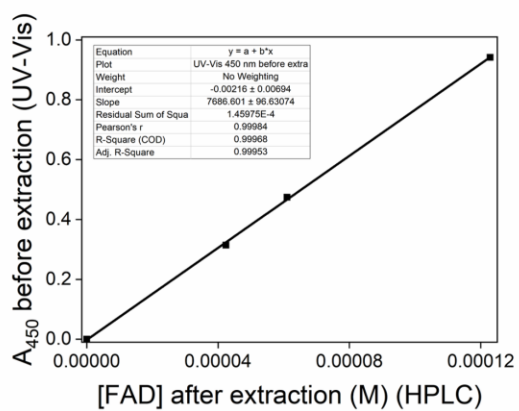


**Fig. S4.** Preparation of GlutOx proteins. Representative (a) Ni-NTA and (b) size exclusion chromatogram and (c) SDS-PAGE analysis. The asterisk in (b) indicates the aggregated form of the recombinant wild type GlutOx, as reported in previous studies.<sup>6</sup> The purified dimeric GlutOx mutants, isolated from SEC fractions, appear as monomers (78 kDa) highlighted with black boxes in (c).

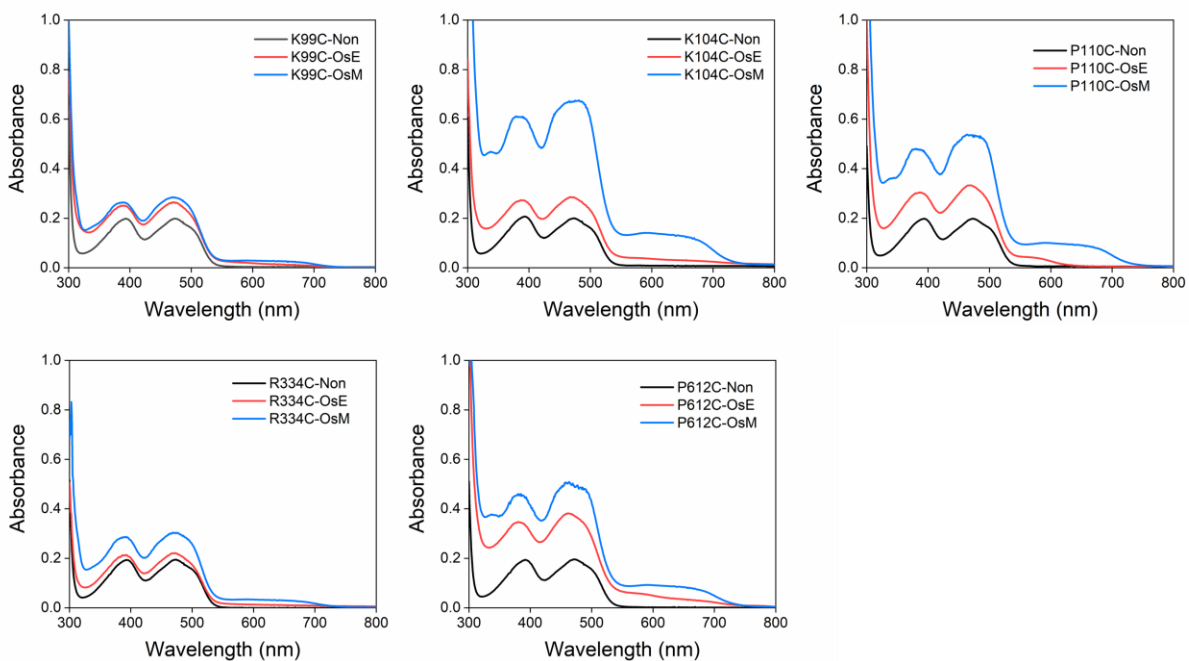
(a)



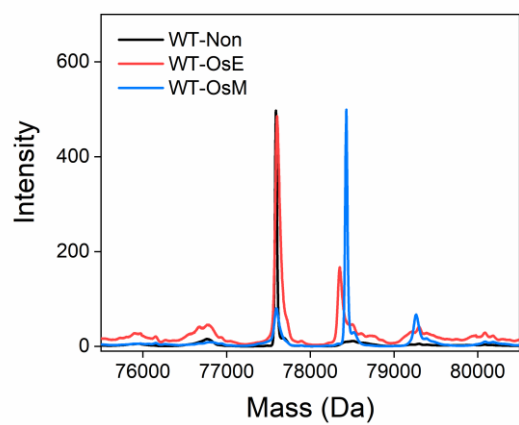
(b)



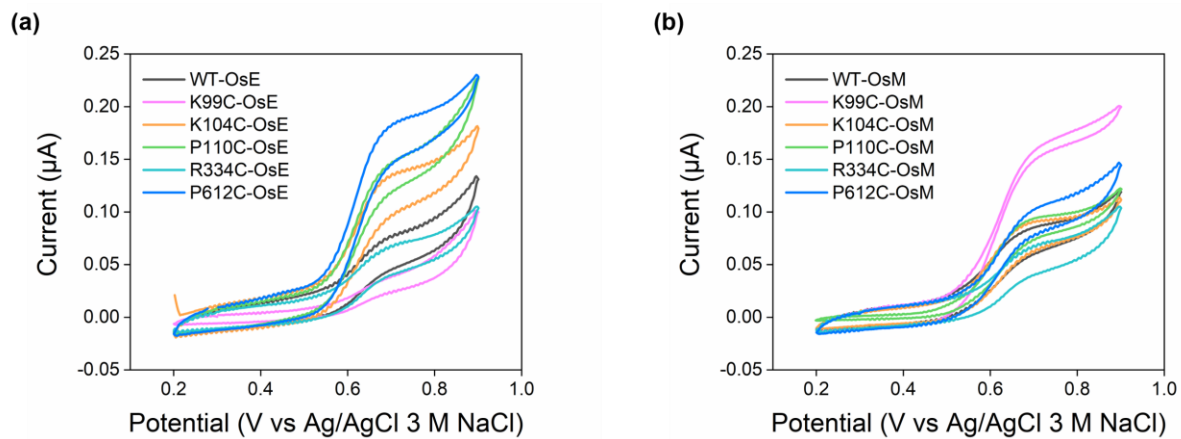
**Fig. S5.** Determination of FAD in GlutOx molar absorptivity. (a) A calibration curve of (a) free FAD and (b) extracted FAD from the wild-type GlutOx protein.



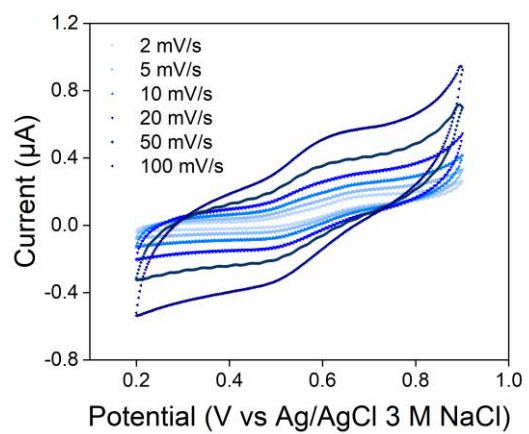
**Fig. S6.** UV-Vis spectra of GlutOx mutants (20  $\mu$ M) before and after conjugation of Os complexes.



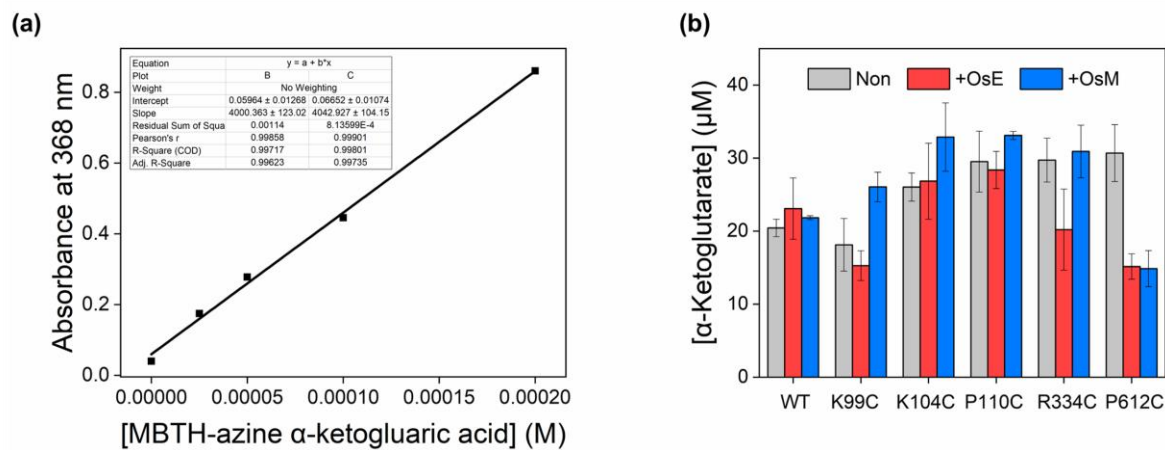
**Fig. S7.** The deconvoluted mass spectra of the Os complexes attached to the wild-type protein.



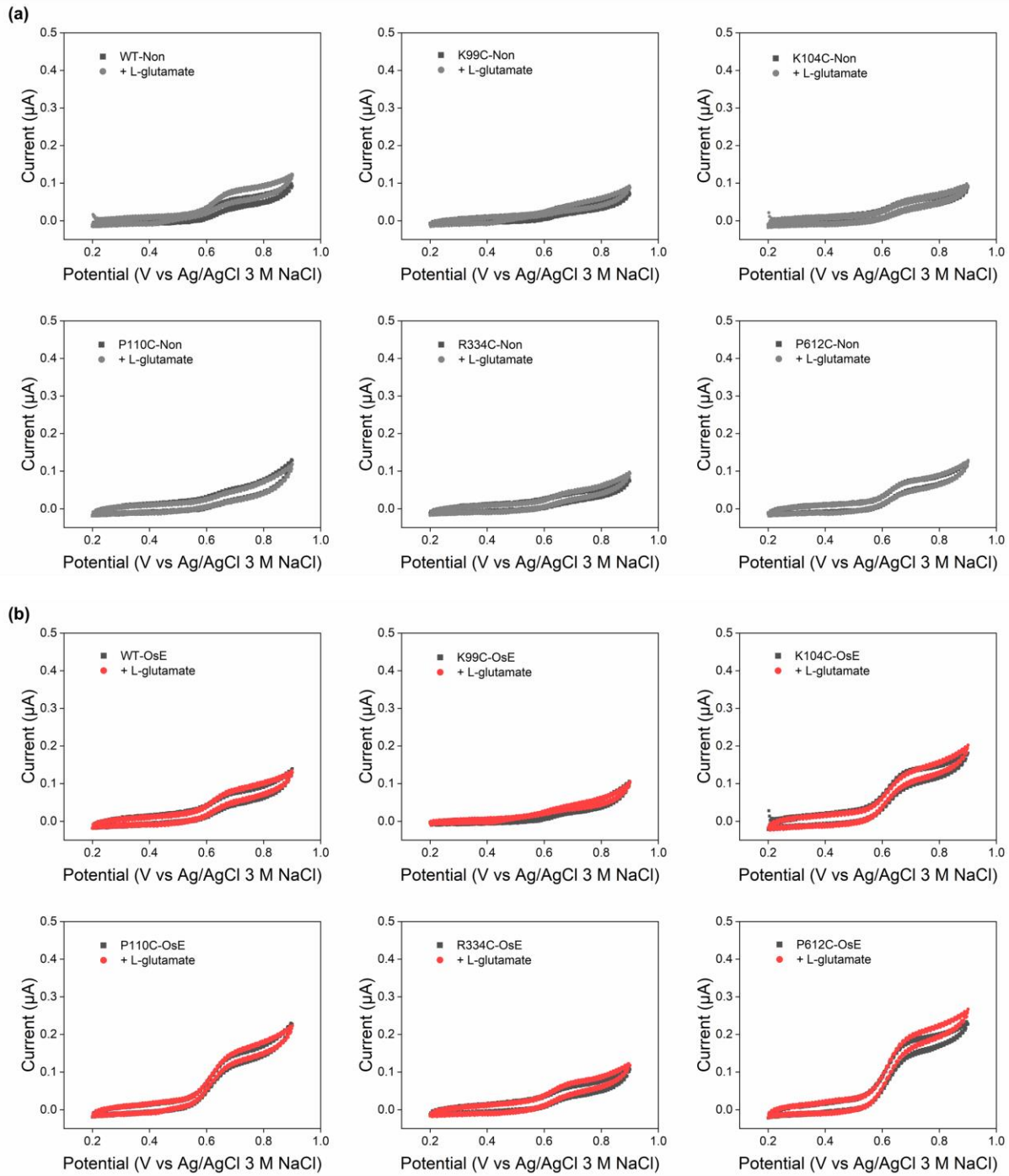
**Fig. S8.** Cyclic voltammograms of OsE- and OsM-bound wild type GlutOx protein and GlutOx mutants (10.0–11.7  $\mu\text{M}$ ) in DPBS (pH 7.4) (scan rate: 2 mV/s).



**Fig. S9.** Cyclic voltammograms of OsM-attached wild-type GlutOx (80 μM) in DPBS (pH 7.4) buffer at various scan rates.



**Fig. S10.** MBTH assay. (a) Determination of molar absorptivity of MBTH-azine  $\alpha$ -ketoglutaric acid (b) Quantification of  $\alpha$ -ketoglutarate production for 15 min.



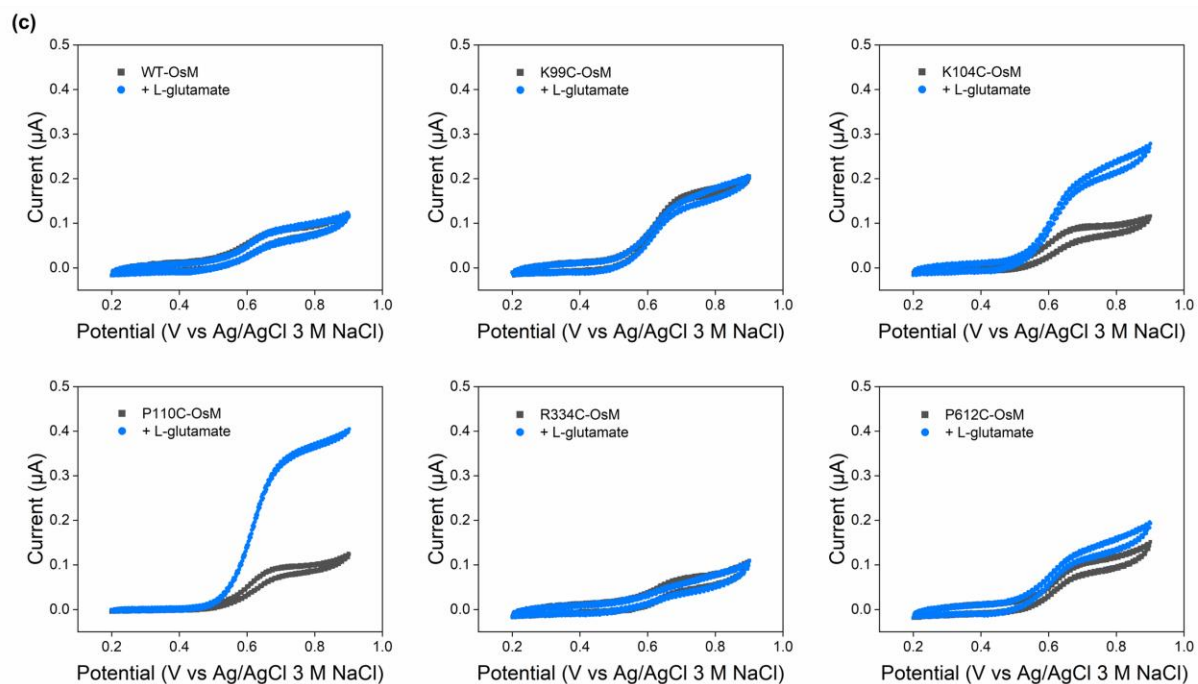


**Fig. S11.** Cyclic voltammograms of glutamate oxidation without secondary redox mediator. (a) Non-conjugated (b) OsE-conjugated (c) OsM-conjugated GlutOx proteins. The black curves represent the diffusion-limited current of GlutOx (10  $\mu\text{M}$ ) in DPBS (pH 7.4). The grey, red, and blue curves represent the catalytic current after the addition of L-glutamate (200 mM).

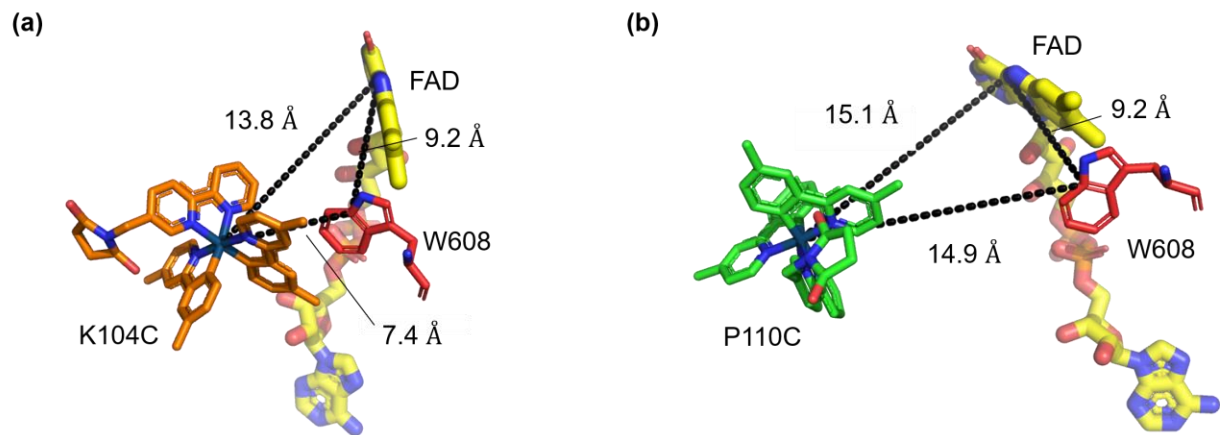


**Fig. S12.** Structural models of OsM-bound (a) K104C and (b) P110C mutants. The coordinates of OsM and GlutOx were adapted and modified from the structure of Ir polypyridyl complex with a maleimide linker (PDB 7YLK) and the wild-type protein (PDB 2E1M). FAD and W608 residue are illustrated with yellow and red sticks, respectively.

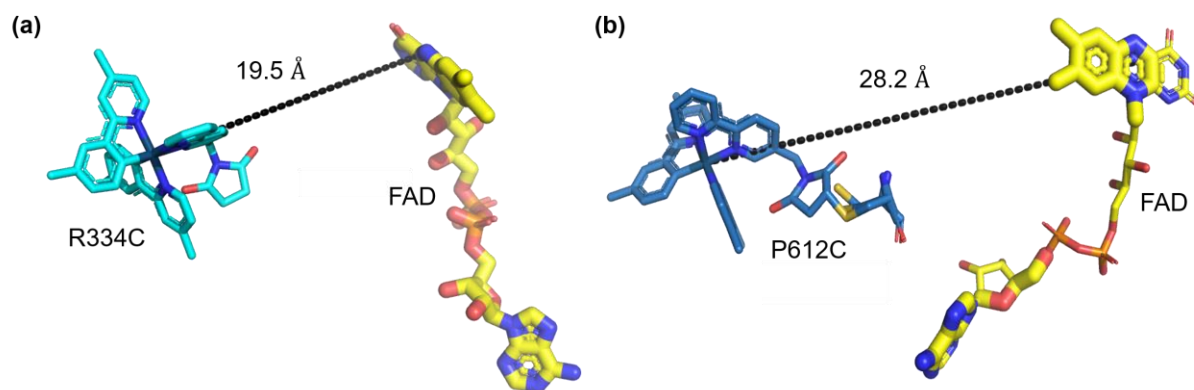


**Fig. S13.** Structural models of OsM-bound GlutOx mutants. (a) R334C and (b) P612C. The steric hindrance near the K99 region disabled us to build the structural model of OsM-bound K99C. The coordinates of OsM and GlutOx were adapted and modified from the structure of Ir polypyridyl complex with a maleimide linker (PDB 7YLK) and the wild-type protein (PDB 2E1M). FAD is shown with yellow stick.

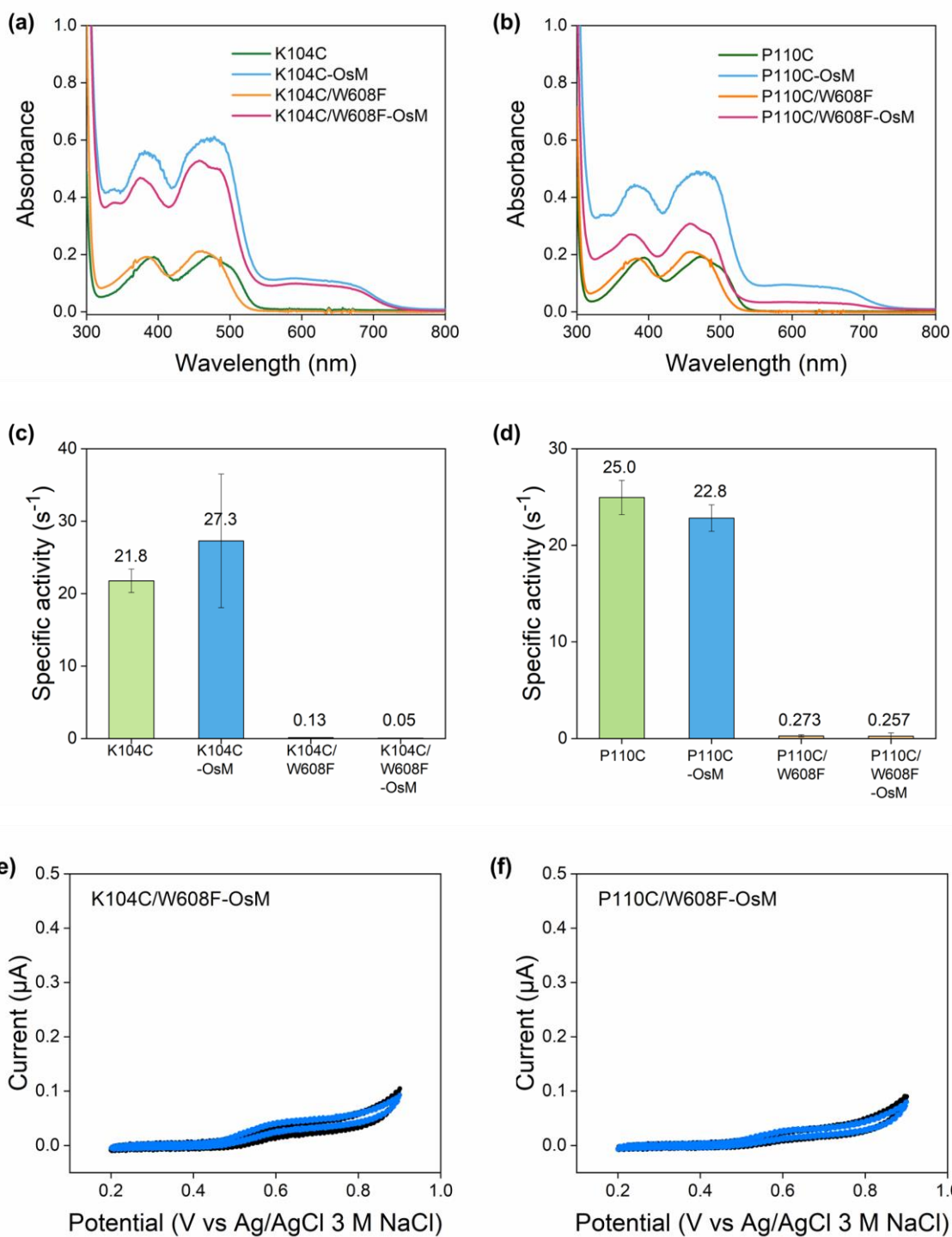
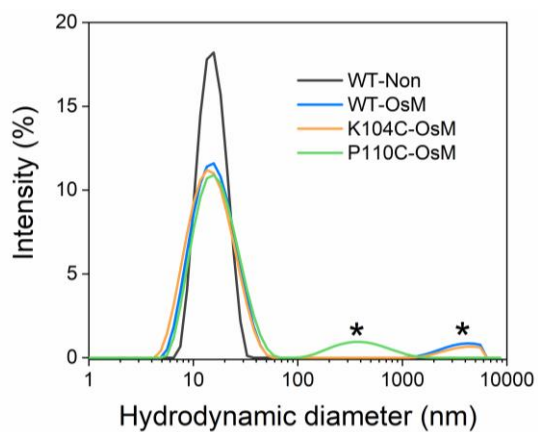


**Fig. S14.** Characterization of tryptophan mutants. UV-Vis spectra of (a) K104C/W608F and (b) P110C/W608F mutants before and after conjugation of OsM. HRP assays of (c) K104C/W608F and (d) P110C/W608F mutants before and after OsM conjugation. Cyclic voltammograms of (e) K104C/W608F and (f) P110C/W608F mutants in the absence and presence of L-glutamate (200 mM) in DPBS (pH 7.0), colored in black and blue, respectively.

(a)



(b)

	Intensity (nm)	Volume (nm)
WT-Non	$16.1 \pm 0.8$	$12.4 \pm 0.1$
WT-OsM	$17.2 \pm 1.1$	$10.7 \pm 0.6$
K104C-OsM	$16.5 \pm 1.2$	$10.7 \pm 0.1$
P110C-OsM	$17.8 \pm 0.6$	$11.1 \pm 0.2$

**Fig. S15.** DLS measurement of GlutOx samples (a) DLS intensity-based size distributions and (b) hydrodynamic diameter determined by intensity or volume. The asterisk in (a) indicates unidentified impurities, whose size varies across different measurements.

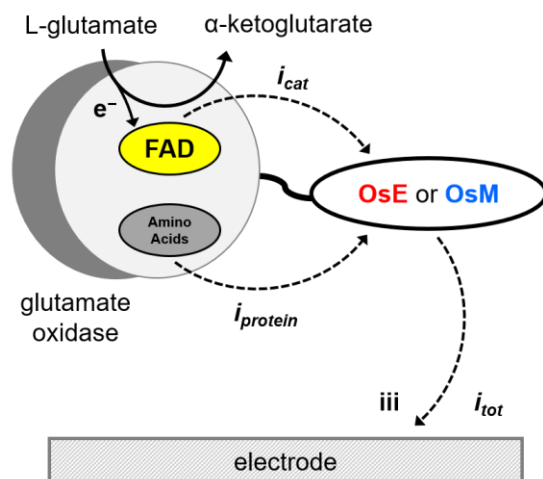


**Fig. S16.** Contributions to the total current in pathway **iii** ( $i_{tot}$ ). The oxidation of active site cofactor (FAD) and electroactive amino acids near the bound osmium are represented as  $i_{cat}$  and  $i_{protein}$ , respectively.

**Table S1.** The amino acid sequence and codon-optimized nucleotide sequence of glutamate Oxidase (GlutOx) from *Streptomyces* sp.X 119-6.

<p><b>Amino acid sequence:</b>  MANEMTYEQLARELLLVGPAPTNE DLKLR YLDVLIDNGLNPPGPPKRILIVGAGIAGLV  AGDLLTRAGHDVTILEANANRVGGRIKTFHAKKGEPSPFADPAQYAEAGAMRLPSFHP  LTLALIDKLGLKRRLFFNVDIDPQTGNQDAPVPPVIFYKSFKDGTWTNGAPSPEFKEP  DKRNHTWIRTNREQVRR AQYATDPSSINEGFHLTGCETRLTVSDMVNQALEPVRDYYS  VKQDDGTRVNKPFKEWLAGWADVVRDFDGYSMGRFLREYAEFSDEAVEAIGTIENM  TSRLHLAFFHSFLGRSDIDPRATYWEIEGSRMLPETLAKDLRDQIVMGQRMVRLEY Y  DPGRDGHGELTGPGGPAVAIQTVPEGEPYAATQWTGDLAIVTIPFSSLRFVKVTPPFS  YKKRRAVIETHYDQATKVLLEFSRRWWEFTEADWKRELD A IAPGLYDYYQQWGEDD  AEAALALPQSVRNLP TGLLGAHPSVDES RIGEEQVEYRNSEL RGGVRPATNAYGGGS  TTDNPNRFMYYP SHPVPGTQGGV VLAAYSWSDDAARWDSFDDAERYGYALENLQSV  HGRRIEVFYTGAGQTQSWLRDPYACGEAAVYTPHQMTAFHLDVVRPEGPVYFAGEHV  SLKHAWIEGAVETA VRAAIAVNEAPV GDTGV TAAAGRRGAAAATEPMREALTSAAA  LEHHHHHH</p>
<p><b>Nucleotide sequence:</b>  CATATGGCCAATGAAATGACCTATGAACAGCTGGCCCGCGAACTGCTGCTGGTTGG  CCCGGCACCGACCAATGAAGATCTGAAACTGCGTTATCTGGATGTGCTGATTGATAA  TGGCCTGAATCCGCCGGGCCCGCCGAAACGTATTCTGATTGTTGGTGCCGGTATTGC  AGGCCTGGTTGCAGGCGATCTGCTGACCCGTGCCGGTCATGATGTTACCATTCTGG  AAGCAAATGCCAATCGTGTGGTGGCCGTATTAAGACCTTTCATGCCAAAAAAGGC  GAACCGAGTCCGTTTGCAGATCCGGCCAGTATGCCGAAGCAGGTGCCATGCGCCT  GCCGAGCTTTCATCCGCTGACCCTGGCCCTGATTGATAAACTGGGCCTGAAACGCC  GTCTGTTTTTCAATGTTGATATTGATCCGCAGACCGGCAATCAGGATGCCCCGGTTC  CGCCGGTTTTCTATAAAAGCTTTAAAGATGGTAAAACCTGGACCAATGGCGCCCCG  AGTCCGGAATTC AAAGAACCGGATAAACGCAATCATACTGGATTTCGCACCAATCG  CGAACAGGTGCGTTCGTGCACAGTATGCCACCGATCCGAGTAGTATTAATGAAGGTT  TTCATCTGACCGGCTGCGAAACCCGTCTGACCGTTAGTGATATGGTTAATCAGGCC  TGGAACCGGTTCTGTGATTATTATAGCGTTAAACAGGATGATGGTACCCGCGTGAATA  AGCCGTTTAAAGAATGGCTGGCCGGCTGGGCAGATGTGGTGCGTGATTTTGATGGC  TATAGTATGGGCCGCTTTCTGCGTGAATATGCAGAATTTTCTGATGAAGCAGTTGAA  GCAATTGGTACCATTGAAAATATGACCAGTCGTCTGCATCTGGCATTTTTCCATAGTT  TTCTGGGCCGTAGCGATATTGATCCTCGCGCCACCTATTGGGAAATTGAAGGCGGTA  GCCGTATGCTGCCGAAACCCTGGCCAAAGATCTGCGCGATCAGATTGTGATGGGT  CAGCGTATGGTGCGCTGGAATATTATGATCCGGGTCGCGATGGTCATCATGGCGAA  CTGACCGGTCCGGGTGGTCCGGCAGTGGCAATTCAGACCGTGCCGGAAGGTGAAC  CGTATGCAGCAACCCAGACCTGGACCGGTGACCTGGCAATTGTGACCATTCCGTTT  AGCAGCTGCGCTTTGTGAAAGTGACCCCGCCGTTTAGCTATAAAAAACGCCGCGC  CGTGATTGAAACCCATTATGATCAGGCAACCAAAGTTCTGCTGGAATTTTACGCC  GCTGGTGGGAATTC ACTGAAGCAGATTGGAAACGTGAACTGGATGCCATTGCCCCG  GGCCTGTATGATTATTATCAGCAGTGGGGTGAAGATGATGCAGAAGCCGCACTGGC  ACTGCCG CAGAGTGTTCGCAATCTGCCGACCGGCCCTGCTGGGTGCACATCCGAGCG  TTGATGAAAGCCGCATTGGTGAAGAACAGGTTGAATATTATCGTAATAGCGAACTG  CGTGGTGGCGTGCGCCCGGCAACCAATGCCTATGGCGGCGGTAGCACCACCGATAA</p>

TCCGAATCGTTTTATGTATTATCCGAGTCATCCGGTCCGGGCACCCAGGGTGGTGT  
GGTTCTGGCCGCATATAGTTGGAGTGATGATGCCGCCCGTTGGGATAGTTTTGATGA  
TGCAGAGCGTTATGGTTATGCCCTGGAAAATCTGCAGAGTGTGCATGGTCGCCGTAT  
TGAAGTGTTTTATAACCGGTGCCGGCCAGACCCAGAGTTGGCTGCGTGATCCGTATG  
CCTGTGGTGAAGCAGCAGTTTATACCCCGCATCAGATGACCGCATTTCATCTGGATG  
TGGTTCGCCCGGAAGGTCCGGTGTATTTGCAGGCGAACATGTTAGCCTGAAACAT  
GCATGGATTGAAGGTGCAGTGGAAACCGCCGTTTCGTGCCGCCATTGCAGTGAATGA  
AGCCCCGGTTGGTGACACCGGTGTTACCGCAGCCGGTCGTCGCGGTGCTGCA  
GCAGCAACCGAACCGATGCGTGAAGAAGCCCTGACCAGCGCGGCCGCACTCGAGC  
ACCACCACCACCACCTGA

**Table S2.** Sequence of primers used for the site-directed mutagenesis.

Mutation	Sequence of primer
C22S	5'- CTG ACC GGC AGC GAA ACC CG -3' 5'- CG GGT TTC GCT GCC GGT CAG -3'
C615S	5'- GAT CCG TAT GCC AGT GGT GAA GCA G -3' 5'- C TGC TTC ACC ACT GGC ATA CGG ATC -3'
K99C	5'- GGC CGT ATT TGC ACC TTT CAT GCC -3' 5'- GGC ATG AAA GGT GCA AAT ACG GCC -3'
K99S	5'- GGC CGT ATT AGC ACC TTT CAT GCC -3' 5'- GGC ATG AAA GGT GCT AAT ACG GCC -3'
K104C	5'- C TTT CAT GCC TGC AAA GGC GAA CCG -3' 5'- CGG TTC GCC TTT GCA GGC ATG AAA G -3'
P110C	5'- GC GAA CCG AGT TGC TTT GCA GAT C -3' 5'- G ATC TGC AAA GCA ACT CGG TTC GC -3'
R334C	5'- GGC GGT AGC TGT ATG CTG CCG -3' 5'- CGG CAG CAT ACA GCT ACC GCC -3'
P612C/C615S	5'- G CGT GAT TGC TAT GCC AGT GGT GAA G -3' 5'- C TTC ACC ACT GGC ATA GCA ATC ACG C -3'
W608F	5'- G ACC CAG AGT TTC CTG CGT GAT CC -3' 5'- GG ATC ACG CAG GAA ACT CTG GGT C -3'

**Table S3.** Distances between the C $\beta$  atoms of the selected positions and the C4a atom of FAD measured using the X-ray crystal structure of GlutOx (PDB code 2E1M).

GlutOx	C $\beta$ ...C4a (Å)
Wild-type	35.6
K99C	10.8
K104C	22.0
P110C	19.0
R334C	13.3
P612C	19.4

**Table S4.** Extinction coefficient of the protein-bound OsE and OsM calculated from UV-Vis spectrophotometry and inductively coupled plasma atomic emission spectroscopy (ICP-OES) analysis.

	OsE	OsM
$\epsilon_{450 \text{ nm}} (\text{cm}^{-1}\text{M}^{-1})$	12597	12639
$\epsilon_{600 \text{ nm}} (\text{cm}^{-1}\text{M}^{-1})$	3497	3828

**Table S5.** Characterization of GluxOx proteins. (a) Bioconjugation yields. Steady-state activity measured with GlutOx proteins (b) before and after conjugation of (c) OsE or (d) OsM.

(a)

GlutOx	[OsE]/[FAD] (%)	[OsM]/[FAD] (%)
Wild-type	59.9	95.5
K99C	25.6	43.4
K104C	47.1	103.3
P110C	72.4	98.6
R334C	26.9	21.5
P612C	87.2	64.5

(b)

Non-conjugated	[H <sub>2</sub> O <sub>2</sub> ] (μM)	[α-ketoglutarate] (μM)	[H <sub>2</sub> O <sub>2</sub> ]/[α-ketoglutarate]
Wild-type	17.2 (0.5)	20 (1)	0.84 (0.05)
K99C	15 (1)	18 (4)	0.82 (0.17)
K104C	18.1 (0.8)	26 (2)	0.70 (0.06)
P110C	16.8 (0.6)	30 (4)	0.57 (0.08)
R334C	17.9 (1.7)	30 (3)	0.60 (0.08)
P612C	22 (2)	31 (4)	0.7 (0.1)

(c)

OsE-conjugated	[H <sub>2</sub> O <sub>2</sub> ] (μM)	[α-ketoglutarate] (μM)	[H <sub>2</sub> O <sub>2</sub> ]/[α-ketoglutarate]
Wild-type	19.5 (0.5)	23 (4)	0.84 (0.16)
K99C	16.4 (1.6)	15 (2)	1.08 (0.18)
K104C	16.9 (0.7)	27 (5)	0.63 (0.12)
P110C	17.5 (0.1)	28 (3)	0.62 (0.06)
R334C	16 (1)	20 (6)	0.80 (0.23)
P612C	4.8 (0.4)	15 (2)	0.32 (0.05)

(d)

OsM-conjugated	[H <sub>2</sub> O <sub>2</sub> ] (μM)	[α-ketoglutarate] (μM)	[H <sub>2</sub> O <sub>2</sub> ]/[α-ketoglutarate]
Wild-type	19.4 (1.3)	21.8 (0.3)	0.89 (0.06)
K99C	17.8 (0.1)	26 (2)	0.68 (0.05)
K104C	21.9 (0.4)	33(5)	0.7 (0.1)
P110C	20 (1)	33.1 (0.5)	0.60 (0.04)
R334C	20.6 (1.4)	31(4)	0.7 (0.1)
P612C	4.6 (0.8)	15 (2)	0.31 (0.08)

**Table S6.** Rate constant for mediated electron transfer (MET) between free [Os(bpy)<sub>3</sub>]<sup>2+</sup> and various GlutOx proteins during glutamate oxidation.

	$k_{ET}$ ( $\times 10^3 \text{ M}^{-1}\text{s}^{-1}$ )		
	Non-conjugated	OsE-conjugated	OsM-conjugated
Wild-type	2.3	2.3	1.4
K99C	11	10	8.2
K104C	4.0	4.1	7.9
P110C	8.1	7.7	11
R334C	3.3	3.5	2.2
P612C	10	5.0	7.0

## References

1. S. Dwaraknath, N.-H. Tran, T. Dao, A. Colbert, S. Mullen, A. Nguyen, A. Cortez and L. Cheruzel, *J. Inorg. Biochem.*, 2014, **136**, 154-160.
2. Y. Ohsawa, M. K. DeArmond, K. W. Hanck and C. G. Moreland, *J. Am. Chem. Soc.*, 1985, **107**, 5383-5386.
3. V. Cafaro, R. Scognamiglio, A. Viggiani, V. Izzo, I. Passaro, E. Notomista, F. D. Piaz, A. Amoresano, A. Casbarra, P. Pucci and A. Di Donato, *Eur. J. Biochem.*, 2002, **269**, 5689-5699.
4. S. Ruccolo, G. Brito, M. Christensen, T. Itoh, K. Mattern, K. Stone, N. A. Strotman and A. C. Sun, *J. Am. Chem. Soc.*, 2022, **144**, 22582-22588.
5. A. Badia, R. Carlini, A. Fernandez, F. Battaglini, S. R. Mikkelsen and A. M. English, *J. Am. Chem. Soc.*, 1993, **115**, 7053-7060.
6. J. Arima, T. Tamura, H. Kusakabe, M. Ashiuchi, T. Yagi, H. Tanaka and K. Inagaki, *J. Biochem.*, 2003, **134**, 805-812.